Fermilab

FERMILAB-Pub-02-303-T

FERMILAB-PUB-02/303-T
ANL-HEP-PR-02-105

Exclusive Double-Charmonium Production from e^+e^- Annihilation into Two Virtual Photons

Geoffrey T. Bodwin and Jungil Lee

High Energy Physics Division, Argonne National Laboratory, 9700 South Cass Avenue, Argonne, Illinois 60439

Eric Braaten

Physics Department, Ohio State University, Columbus, Ohio 43210 and

Fermi National Accelerator Laboratory, P. O. Box 500, Batavia, Illinois 60510

(Dated: March 27, 2003)

arXiv:hep-ph/0212352 v3 27 Mar 2003

Abstract

We calculate the contributions from QED processes involving two virtual photons to the cross sections for e^+e^- annihilation into two charmonium states with the same C-parity. Generically, the cross sections are three orders of magnitude smaller than those for charmonia with opposite C-parity because they are suppressed by a factor of α^2/α_s^2. However, if both charmonia have quantum numbers $J^{PC} = 1^{--}$, then there is a contribution to the cross section that involves the fragmentation of each photon into a charmonium. The fragmentation contribution is enhanced by powers of $E_{\rm beam}/m_c$, the ratio of the beam energy to the charm-quark mass, and this enhancement can compensate for the suppression factor that is associated with the coupling constants. In particular, the predicted cross section for $J/\psi + J/\psi$ at the B factories is larger than that for $J/\psi + \eta_c$.

PACS numbers: 12.38.-t, 12.38.Bx, 13.20.Gd, 14.40.Gx

I. INTRODUCTION

Recently, the Belle Collaboration observed e^+e^- annihilation into two charmonium states at a center-of-mass energy $\sqrt{s} = 10.6$ GeV by studying the recoil momentum spectrum of the J/ψ [1]. The collaboration measured the cross section for $J/\psi + \eta_c$ and also found evidence for production of $J/\psi + \chi_{c0}$ and $J/\psi + \eta_c(2S)$. With more precise measurements and additional data, it may be possible to discover the D-wave charmonium states $\eta_{c2}(1D)$ and $\psi_2(1D)$ at the B factories by studying the momentum spectra of the J/ψ and other charmonium states.

The exclusive cross sections for double-charmonium states provide stringent tests of the NRQCD factorization method for calculating the cross sections for heavy-quarkonium production [2]. The predictions of the NRQCD factorization method for exclusive double-charmonium production reduce essentially to those of the color-singlet model for quarkonium production [3], up to relativistic corrections that are second order in the relative velocity v of the quark and antiquark in the charmonium. The nonperturbative factors in the NRQCD factorization formula for the cross section in the nonrelativistic limit can be determined phenomenologically from electromagnetic annihilation decay rates. Cross sections for double-charmonium production can therefore be predicted, up to corrections that are suppressed by powers of v^2, without any unknown phenomenological factors.

Recent calculations of the cross section for $J/\psi + \eta_c$ have given results that are about an order of magnitude smaller than the Belle measurement [4, 5]. The relativistic corrections are large, and they may account for part of the discrepancy [4]. It has also been suggested that there may be large nonperturbative corrections to double-charmonium cross sections at the B-factory energy [5].

In this paper, we calculate the cross sections for e^+e^- annihilation into two charmonium states that have the same charge-conjugation parity (C-parity), such as $J/\psi + J/\psi$. These processes proceed, at leading order in the QCD coupling α_s, through QED diagrams with that contain two virtual photons. One might expect that these cross sections would be much smaller than those for charmonia with opposite C-parity because they are suppressed by a factor of α^2/α_s^2. However, if both charmonia have quantum numbers $J^{PC} = 1^{--}$, then there is a contribution to the cross section in which each photon fragments into a charmonium [6]. The fragmentation contribution is enhanced by powers of $E_{\rm beam}/m_c$, where $E_{\rm beam}$ is the beam energy and m_c is the charm-quark mass [6]. This enhancement can compensate for the suppression factor that is associated with the coupling constants. In particular, the predicted cross section for $J/\psi + J/\psi$ at the B factories is larger than that for $J/\psi + \eta_c$.

II. CROSS SECTIONS

In this section, we calculate the contributions from e^+e^- annihilation through two virtual photons to the production cross sections for double-charmonium states $H_1 + H_2$. Charge-conjugation symmetry requires the two charmonia to be either two $C = -1$ states or two $C = +1$ states. We express our results in terms of the ratio $R[H_1 + H_2]$, which is defined by

$$R[H_1 + H_2] = \frac{\sigma[e^+e^- \to H_1 + H_2]}{\sigma[e^+e^- \to \mu^+\mu^-]}, \tag{1}$$

where $\sigma[e^+e^- \to \mu^+\mu^-] = \pi\alpha^2/(3E_{\rm beam}^2)$ and $E_{\rm beam} = \sqrt{s}/2$ is the beam energy in the center-of-momentum (CM) frame. We give the angular distributions dR/dx for each of the

helicity states of H_1 and H_2. The angular variable is $x = \cos\theta$, where θ is the angle between the e^- and H_1 in the e^+e^- CM frame.

A. Asymptotic behavior

The 4 QED diagrams that contribute to the process $e^+e^- \to \gamma^*\gamma^* \to c\bar{c}_1 + c\bar{c}_1$ at order α^4 are shown in Fig. 1. The diagrams in Figs. 1(a) and 1(b) contribute only for charmonia with quantum numbers $J^{PC} = 1^{--}$, such as J/ψ, $\psi(2S)$, and $\psi_1(1D)$. The procedure for calculating the matrix element for $e^+e^- \to H_1(P_1) + H_2(P_2)$ from the matrix element for $e^+e^- \to c(p_1)\bar{c}(\bar{p}_1) + c(p_2)\bar{c}(\bar{p}_2)$ is summarized in Ref. [4].

When the energy $E_{\rm beam}$ is much larger than the charm-quark mass m_c, the relative sizes of the double-charmonium cross sections are governed largely by the number of kinematic suppression factors r^2, where the variable r is defined by

$$r^2 \;=\; \frac{4m_c^2}{E_{\rm beam}^2}. \tag{2}$$

If we set $m_c = 1.4$ GeV and $E_{\rm beam} = 5.3$ GeV, then $r^2 = 0.28$.

The asymptotic behavior of the ratio $R[H_1 + H_2]$ as $r \to 0$ can be determined from the helicity selection rules for exclusive processes in perturbative QCD [7, 8], which apply equally well to QED. For generic charmonia, whose quantum numbers are different from those of the photon, only the diagrams in Figs. 1(c) and 1(d) contribute. There is a suppression factor r^2 for each $c\bar{c}$ pair with small relative momentum in the final state. Thus the ratio $R[H_1(\lambda_1)+H_2(\lambda_2)]$ decreases at least as fast as r^4 as $r \to 0$. This slowest asymptotic decrease can occur only if the sum of the helicities of the charmonia vanishes: $\lambda_1 + \lambda_2 = 0$. For every unit of helicity by which this selection rule is violated, there is a further suppression factor of r^2. Thus the estimate for the ratio R at leading-order in the QED and QCD coupling constants is

$$R[H_1(\lambda_1) + H_2(\lambda_2)] \;\sim\; \alpha^2 (v^2)^{3+L_1+L_2} (r^2)^{2+|\lambda_1+\lambda_2|}. \tag{3}$$

The factor of v^{3+2L} for a charmonium state with orbital angular momentum L comes from the NRQCD matrix elements. At leading order, there may, of course, be further suppression factors of r^2, and the cross section could even vanish. For charmonia with opposite charge conjugation, the estimate for R is given by Eq. (3) with α^2 replaced by α_s^2. Thus, the cross sections for generic charmonia with the same charge conjugation are suppressed compared to those for opposite charge conjugation by a factor of $\alpha^2/\alpha_s^2 \approx 10^{-3}$.

Production cross sections for charmonia with $J^{PC} = 1^{--}$ are an exception to this generic estimate because they also receive contributions from the diagrams in Figs. 1(a) and 1(b), which we will refer to as photon-fragmentation diagrams. These contributions are enhanced because the virtual-photon propagators are of order $1/m_c^2$ instead of order $1/E_{\rm beam}^2$. In the amplitude, there are also two numerator factors of m_c instead of $E_{\rm beam}$, which arise from the $c\bar{c}$ electromagnetic currents. Hence, the net enhancement of the squared amplitude is $(E_{\rm beam}/m_c)^4$, and the contributions to R can be nonzero in the limit $r \to 0$. As $r \to 0$ with fixed scattering angle θ, the photon-fragmentation contributions to the cross section factor into the cross section for $e^+e^- \to \gamma\gamma$ with photon scattering angle θ and the fragmentation probabilities for $\gamma \to H_1$ and $\gamma \to H_2$. These fragmentation probabilities are nonzero

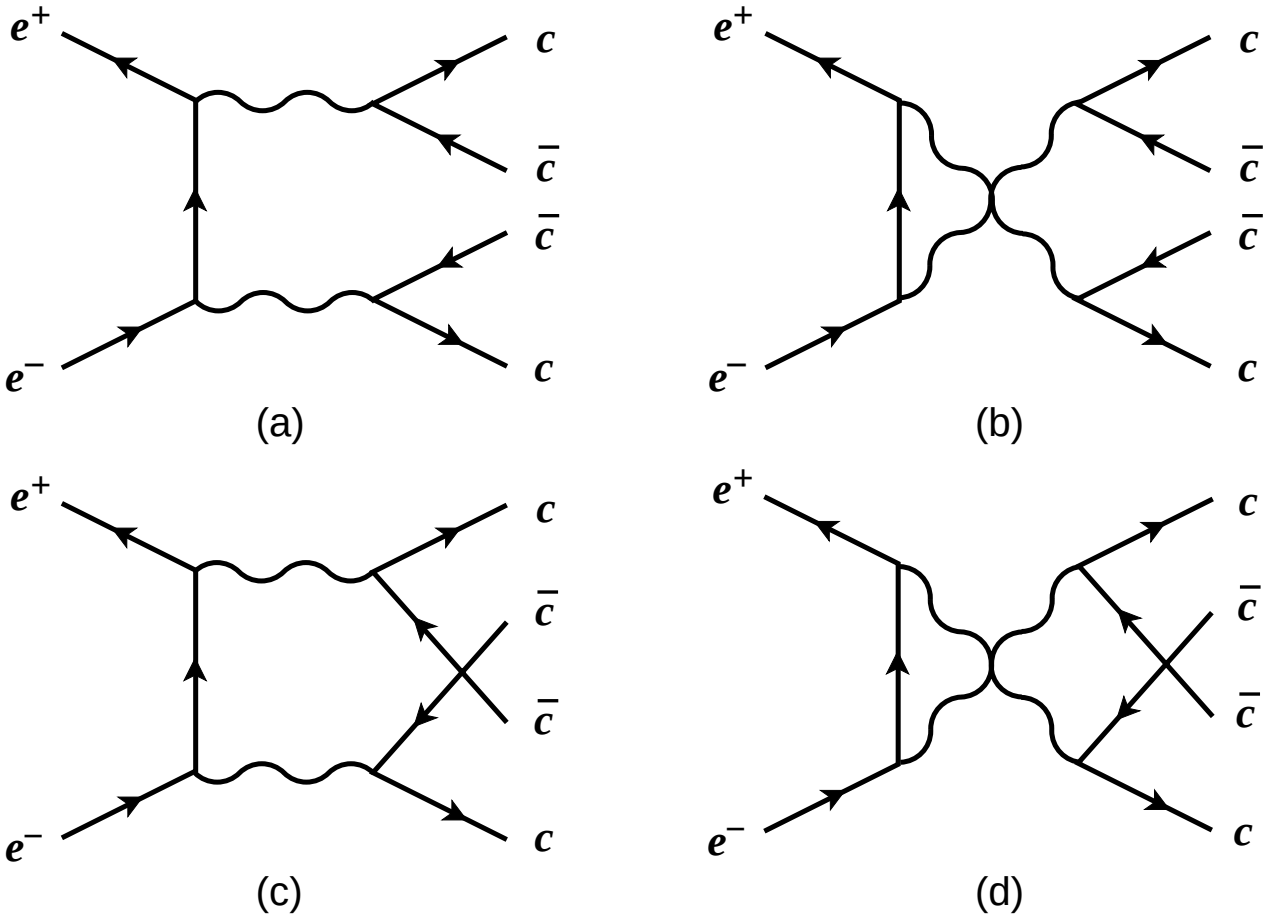

FIG. 1: QED diagrams for the process $e^+e^- \to \gamma^*\gamma^* \to c\bar{c}_1 + c\bar{c}_1$. The upper and lower $c\bar{c}$ pairs evolve into H_1 and H_2, respectively.

at order α only for $J^{PC} = 1^{--}$ states with helicities satisfying $\lambda_1 = -\lambda_2 = \pm 1$. The contribution to the ratio R for $J/\psi + J/\psi$ has the behavior

$$R[J/\psi(\lambda_1) + J/\psi(\lambda_2)] \;\sim\; \alpha^2 (v^2)^3, \qquad \lambda_1 = -\lambda_2 = \pm 1. \tag{4}$$

This estimate applies equally well to $J/\psi + \psi(2S)$ and $\psi(2S) + \psi(2S)$. For $J/\psi + \psi_1(1D)$ and $\psi(2S) + \psi_1(1D)$, there is an additional suppression factor of v^4 from the NRQCD matrix elements. For $\psi_1(1D) + \psi_1(1D)$, the additional suppression factor is v^8.

Using the QCD version of Eq. (3), we obtain the estimate

$$R[J/\psi + \eta_c] \;\sim\; \alpha_s^2 (v^2)^3 (r^2)^3, \tag{5}$$

which holds generally for S-wave final states with opposite C-parity. The ratio R in Eq. (4) is suppressed relative to Eq. (5) by a factor of $(\alpha/\alpha_s)^2 \approx 10^{-3}$, but the enhancement factor that scales as r^{-6} makes the cross sections comparable in magnitude at the energy of a B factory.

B. *S*-wave + *S*-wave

The cross section for $\eta_c + \eta_c$ receives contributions only from the nonfragmentation diagrams in Figs. 1(c) and 1(d). The angular distribution is

$$\frac{dR}{dx}[\eta_c + \eta_c] = \frac{\pi^2 e_c^4 \alpha^2}{3}\, x^2(1-x^2)\, r^4(1-r^2)^{5/2}\, \frac{\langle O_1\rangle_{\eta_c}\langle O_1\rangle_{\eta_c}}{m_c^6}. \tag{6}$$

The total ratio R for $\eta_c + \eta_c$ is obtained by integrating over x only from 0 to 1 in order to avoid double-counting of the identical final-state particles:

$$R[\eta_c + \eta_c] = \frac{2\pi^2 e_c^4 \alpha^2}{45}\, r^4(1-r^2)^{5/2}\, \frac{\langle O_1\rangle_{\eta_c}\langle O_1\rangle_{\eta_c}}{m_c^6}. \tag{7}$$

Note that the ratio (7) depends on the charm-quark mass m_c explicitly and also through the variable r defined in Eq. (2). One of the factors of $(1-r^2)^{1/2}$ in Eq. (7) is the nonrelativistic limit of the phase-space factor $P_{\rm CM}/E_{\rm beam}$, where $P_{\rm CM}$ is the momentum of either charmonium in the center-of-momentum frame. It can be expressed as

$$\frac{P_{\rm CM}}{E_{\rm beam}} = \frac{\lambda^{1/2}(s, M_{H_1}^2, M_{H_2}^2)}{s}, \tag{8}$$

where $\lambda(x,y,z) = x^2 + y^2 + z^2 - 2(xy + yz + zx)$ and M_{H_i} is the mass of H_i.

The angular distribution dR/dx for $\eta_c + \eta_c(2S)$ is given by an expression identical to Eq. (6), except that one of the factors of $\langle O_1\rangle_{\eta_c}$ is replaced by $\langle O_1\rangle_{\eta_c(2S)}$. Since the two final-state particles are distinguishable, the total ratio R for $\eta_c + \eta_c(2S)$ is obtained by integrating over x from -1 to 1. Thus, the total ratio R for $\eta_c + \eta_c(2S)$ is obtained from Eq. (7) by replacing one of the factors of $\langle O_1\rangle_{\eta_c}$ by $\langle O_1\rangle_{\eta_c(2S)}$ and multiplying by a factor 2.

The cross section for $J/\psi + J/\psi$ receives contributions from all four diagrams in Fig. 1, including the photon-fragmentation diagrams. The angular distribution dR/dx is

$$\frac{dR}{dx}[J/\psi(\lambda_1) + J/\psi(\lambda_2)] = \frac{\pi^2 e_c^4 \alpha^2}{3}\, \frac{F(\lambda_1,\lambda_2,x)(1-r^2)^{1/2}}{[4(1-r^2)(1-x^2)+r^4]^2}\, \frac{\langle O_1\rangle_{J/\psi}\langle O_1\rangle_{J/\psi}}{m_c^6}, \tag{9}$$

where the entries of $F(\lambda_1,\lambda_2,x)$ are

$$F(0,0,x) = r^4x^2(1-x^2)[10 - 3r^4 + r^6 - 4x^2(1-r^4)]^2, \tag{10a}$$

$$F(\pm1,\mp1,x) = (1+x^2)(1-x^2)[6 + r^2 - 4r^4 + r^6 - 4x^2r^2(1-r^2)]^2, \tag{10b}$$

$$F(\pm1,\pm1,x) = r^4x^2(1-x^2)[3 + 4r^2 - 4r^4 + r^6 - 4x^2r^2(1-r^2)]^2, \tag{10c}$$

$$F(\pm1,0,x) = F(0,\pm1,x) = (r^2/4)[f^2(x) + f^2(-x)]. \tag{10d}$$

The function $f(x)$ in Eq. (10d) is defined by

$$f(x) = (1+x)\big[(1-2x)(1+r^2)(2-r^2)(3-r^2) + 6x(1-r^2) - 4x^2(1-2x)r^2(1-r^2)\big]. \tag{11}$$

The total ratio R is obtained by summing over the helicities λ_1 and λ_2 and integrating over x only from 0 to 1. The resulting expression is so complicated that it is not very useful to write it down. The ratio dR/dx for $J/\psi + \psi(2S)$ is given by an expression identical to

Eq. (9), except that one of the factors of $\langle O_1\rangle_{J/\psi}$ is replaced by $\langle O_1\rangle_{\psi(2S)}$ and the range of x is from -1 to 1.

In the limit $r \to 0$ with x fixed, only the transverse helicity states $\lambda_1 = -\lambda_2 = \pm 1$ in Eq. (10b) contribute. The angular distribution dR/dx summed over helicities reduces in this limit to

$$\frac{dR}{dx}[J/\psi(\pm 1) + J/\psi(\mp 1)] \approx \frac{3(1+x^2)}{2(1-x^2)}\, P^2_{\gamma\to J/\psi}, \tag{12}$$

where $P_{\gamma\to J/\psi}$ is the probability for a photon to fragment into a J/ψ [9]:

$$P_{\gamma\to J/\psi} = e_c^2 \pi\alpha \frac{\langle O_1\rangle_{J/\psi}}{m_c^3}. \tag{13}$$

The coefficient of $P^2_{\gamma\to J/\psi}$ in Eq. (12) is dR/dx for the process $e^+e^- \to \gamma\gamma$. The differential ratio (12) is compatible with the asymptotic form (4). However the integrated cross section is enhanced by a factor $\ln(8/r^4)$, relative to Eq. (4). The logarithmic factor arises because, as can be seen from Eq. (9), the potential divergence at $x = \pm 1$ in the integral of Eq. (12) is cut off at $1 \pm x \sim r^4/8$.

Chang, Qiao, and Wang have pointed out that the cross sections for $e^+e^- \to J/\psi + \gamma$ is also large if $E_{\rm beam} \gg m_c$ [10]. The reason is that this process has a fragmentation contribution that factors into the short-distance cross section for $e^+e^- \to \gamma\gamma$ and a single fragmentation probability $P_{\gamma\to J/\psi}$. The ratio dR/dx for this process therefore has a finite limit as $r \to 0$, and the cross section is sharply peaked near the beam direction.

C. *S*-wave + *P*-wave

The cross section for $J/\psi + h_c$ receives contributions only from the nonfragmentation diagrams in Figs. 1(c) and 1(d). The angular distribution is

$$\frac{dR}{dx}[J/\psi(\lambda_1) + h_c(\lambda_2)] = \frac{\pi^2 e_c^4 \alpha^2}{24}\, G(\lambda_1,\lambda_2,x)\, r^4 (1-r^2)^{3/2}\, \frac{\langle O_1\rangle_{J/\psi}\langle O_1\rangle_{h_c}}{m_c^8}, \tag{14}$$

where the non-zero entries of $G(\lambda_1,\lambda_2,x)$ are

$$G(0,0,x) = 2(1-x^2), \tag{15a}$$
$$G(0,\pm 1,x) = r^2(1-3x^2+4x^4), \tag{15b}$$
$$G(\pm 1,\mp 1,x) = 8(1-x^4), \tag{15c}$$
$$G(\pm 1,0,x) = 4r^2x^2(1+x^2). \tag{15d}$$

The total ratio R is obtained by summing over the helicities λ_1 and λ_2 and integrating over x from -1 to 1:

$$R[J/\psi + h_c] = \frac{\pi^2 e_c^4 \alpha^2}{45}\, r^4 (53 + 22r^2)(1-r^2)^{3/2}\, \frac{\langle O_1\rangle_{J/\psi}\langle O_1\rangle_{h_c}}{m_c^8}. \tag{16}$$

The cross section for $\eta_c + \chi_{cJ}$ receives contributions only from the nonfragmentation diagrams in Figs. 1(c) and 1(d). The angular distribution is

$$\frac{dR}{dx}[\eta_c + \chi_{cJ}(\lambda_2)] = \frac{2\pi^2 e_c^4 \alpha^2}{27}\, G_J(\lambda_2,x)\, r^4 (1-r^2)^{3/2}\, \frac{\langle O_1\rangle_{\eta_c}\langle O_1\rangle_{\chi_{cJ}}}{m_c^8}, \tag{17}$$

where the non-zero entries of $G_J(\lambda_2, x)$ are

$$G_0(0,x) = (3/4)(1-x^2), \tag{18a}$$
$$G_1(0,x) = 9x^2(1-x^2), \tag{18b}$$
$$G_1(\pm 1,x) = (9r^2/32)(1+x^2+16x^4), \tag{18c}$$
$$G_2(0,x) = (3/4)(1-x^2), \tag{18d}$$
$$G_2(\pm 1,x) = (9r^2/32)(1+x^2). \tag{18e}$$

The total ratio R is obtained by summing over the helicities λ_1 and λ_2 and integrating over x from -1 to 1:

$$R[\eta_c + \chi_{cJ}] = \frac{2\pi^2 e_c^4 \alpha^2}{27} G_J \, r^4 (1-r^2)^{3/2} \, \frac{\langle O_1 \rangle_{\eta_c} \langle O_1 \rangle_{\chi_{cJ}}}{m_c^8}, \tag{19}$$

where the coefficients G_J are

$$G_0 = 1, \tag{20a}$$
$$G_1 = (3/10)(8+17r^2), \tag{20b}$$
$$G_2 = (1/2)(2+3r^2). \tag{20c}$$

D. *P*-wave + *P*-wave

The cross section for $h_c + h_c$ receives contributions only from the nonfragmentation diagrams in Figs. 1(c) and 1(d). The angular distribution is

$$\frac{dR}{dx}[h_c(\lambda_1) + h_c(\lambda_2)] = \frac{\pi^2 e_c^4 \alpha^2}{24} H(\lambda_1, \lambda_2, x) \, r^4 (1-r^2)^{1/2} \, \frac{\langle O_1 \rangle_{h_c} \langle O_1 \rangle_{h_c}}{m_c^{10}}, \tag{21}$$

where the functions $H(\lambda_1, \lambda_2, x)$ are

$$H(0,0,x) = 2x^2(1-x^2)[4-6r^2+3r^4-4x^2(1-r^2)]^2, \tag{22a}$$
$$H(\pm 1, \mp 1, x) = h_1(x) + h_1(-x), \tag{22b}$$
$$H(\pm 1, 0, x) = H(0, \pm 1, x) = h_2(x) + h_2(-x), \tag{22c}$$
$$H(\pm 1, \pm 1, x) = (r^4/2)x^2(1-x^2)[1+(5-4x^2)(1-r^2)]^2. \tag{22d}$$

The functions $h_i(x)$ in Eqs. (22b) and (22c) are defined by

$$h_1(x) = (1/4)(1+x)^2(1-x^2)[(2-r^2)^2 + 4x(1-x)r^2(1-r^2)]^2, \tag{23a}$$
$$h_2(x) = (r^2/8)(1-x)^2[(1+2x)(2-r^2) - 8x^2(1+x)(1-r^2)]^2. \tag{23b}$$

The total ratio R is obtained by summing over the helicities λ_1 and λ_2 and integrating over x from 0 to 1:

$$R[h_c + h_c] = \frac{\pi^2 e_c^4 \alpha^2}{3780} (2272 - 3880r^2 + 3300r^4 - 2158r^6 + 781r^8) \times r^4 (1-r^2)^{1/2} \, \frac{\langle O_1 \rangle_{h_c} \langle O_1 \rangle_{h_c}}{m_c^{10}}. \tag{24}$$

We have not calculated the cross sections for $\chi_{cJ} + \chi_{cJ'}$. They receive contributions only from the nonfragmentation diagrams in Figs. 1(c) and 1(d). We therefore expect them to be comparable to the cross section for $h_c + h_c$.

E. *S*-wave + *D*-wave

The cross section for $\eta_c + \eta_{c2}$ receives contributions only from the nonfragmentation diagrams in Figs. 1(c) and 1(d). The angular distribution is

$$\frac{dR}{dx}[\eta_c + \eta_{c2}(\lambda_2)] = \frac{\pi^2 e_c^4 \alpha^2}{288}\, I(\lambda_2, x)\, r^4 (1-r^2)^{1/2}\, \frac{\langle O_1\rangle_{\eta_c}\langle O_1\rangle_{\eta_{c2}}}{m_c^{10}}, \tag{25}$$

where the functions $I(\lambda_2, x)$ are

$$\begin{aligned}
I(0,x) &= x^2(1-x^2)[4-8r^2+5r^4+4x^2(1-r^2)(2-r^2)]^2, && \text{(26a)}\\
I(\pm 1,x) &= i_1(x) + i_1(-x), && \text{(26b)}\\
I(\pm 2,x) &= i_2(x) + i_2(-x). && \text{(26c)}
\end{aligned}$$

The functions $i_i(x)$ in Eqs. (26b) and (26c) are defined by

$$\begin{aligned}
i_1(x) &= (3r^2/4)(1-x)^2[2-3r^2-2xr^2-8x^2(1+x)(1-r^2)]^2, && \text{(27a)}\\
i_2(x) &= (3r^4/4)(1-x^2)(1-x)^2[1+(1-r^2)(1+2x)^2]^2. && \text{(27b)}
\end{aligned}$$

Then total ratio R is obtained by summing over the helicities λ_2 and integrating over x from -1 to 1:

$$\begin{aligned}
R[\eta_c + \eta_{c2}] &= \frac{\pi^2 e_c^4 \alpha^2}{22680}\,(1232 - 3048r^2 + 4880r^4 - 3726r^6 + 1439r^8)\\
&\quad \times r^4(1-r^2)^{1/2}\, \frac{\langle O_1\rangle_{\eta_c}\langle O_1\rangle_{\eta_{c2}}}{m_c^{10}}. && \text{(28)}
\end{aligned}$$

The cross section for $J/\psi + \psi_1$ receives contributions from all four diagrams in Fig. 1, including the photon fragmentation diagrams. The angular distribution is

$$\frac{dR}{dx}[J/\psi(\lambda_1) + \psi_1(\lambda_2)] = \frac{\pi^2 e_c^4 \alpha^2}{5760}\, \frac{J(\lambda_1, \lambda_2, x)\,(1-r^2)^{1/2}}{[4(1-r^2)(1-x^2)+r^4]^2}\, \frac{\langle O_1\rangle_{J/\psi}\langle O_1\rangle_{\psi_1}}{m_c^{10}}, \tag{29}$$

where the functions $J(\lambda_1, \lambda_2, x)$ are

$$\begin{aligned}
J(0,0,x) &= 2\,r^4\,x^2\,(1-x^2)\,\big[228 - 124r^2 + 158r^4 - 101r^6 + 22r^8 - 4x^2(1-r^2)\\
&\quad \times(34 - 37r^2 + 34r^4 - 2r^6) + 32x^4(1-r^2)^2(2-r^2)\big]^2, && \text{(30a)}\\
J(\pm 1, \mp 1, x) &= j_{+-}(x) + j_{+-}(-x), && \text{(30b)}\\
J(\pm 1, 0, x) &= j_{+0}(x) + j_{+0}(-x), && \text{(30c)}\\
J(0, \pm 1, x) &= j_{0+}(x) + j_{0+}(-x), && \text{(30d)}\\
J(\pm 1, \pm 1, x) &= j_{++}(x) + j_{++}(-x). && \text{(30e)}
\end{aligned}$$

The functions $j_{\lambda\lambda'}(x)$ are defined by

$$\begin{aligned}
j_{+-}(x) &= (1/4)(1-x^2)(1-x)^2\big[3(2-r^2)(52-16r^2+38r^4-11r^6-2r^8) \\
&\quad -24xr^4(2-r^2)^2(1-r^2)+4x^2r^2(1-r^2)(40-85r^2+22r^4-6r^6) \\
&\quad +96x^3r^4(1-r^2)^2-32x^4r^2(1-r^2)^2(2-3r^2)\big]^2, \qquad (31a) \\
j_{+0}(x) &= (r^2/8)(1-x)^2\big[(2-r^2)(156+28r^2+24r^4-19r^6) \\
&\quad +2x(156+56r^2-4r^4-38r^6+13r^8)-4x^2r^2(1-r^2)(46-13r^2+8r^4) \\
&\quad -8x^3r^2(1-r^2)(22+5r^2+2r^4)+128x^4r^2(1-r^2)^2+64x^5r^2(1-r^2)^2\big]^2, \qquad (31b) \\
j_{0+}(x) &= (r^2/8)(1+x)^2\big[(2-r^2)(156+40r^2-18r^4-r^6) \\
&\quad -2x(156-28r^2+164r^4-143r^6+34r^8)-4x^2r^2(1-r^2)(52-31r^2+8r^4) \\
&\quad +8x^3r^2(1-r^2)(1+26r^2+2r^4)+128x^4r^2(1-r^2)^2-64x^5r^2(1-r^2)^2\big]^2, \qquad (31c) \\
j_{++}(x) &= (r^4/4)(1-x^2)\big[32x^5r^2(1-r^2)^2-4x^3r^2(1-r^2)(57-30r^2+2r^4) \\
&\quad -24x^2r^2(1-r^2)+x(156+196r^2-284r^4+137r^6-22r^8) \\
&\quad +6r^2(2-r^2)^2\big]^2. \qquad (31d)
\end{aligned}$$

The total ratio R is obtained by summing over the helicities λ_1 and λ_2 and integrating x from -1 to 1.

We have not calculated the cross section for $J/\psi+\psi_2(1D)$. It receives contributions only from the nonfragmentation diagrams in Figs. 1(c) and 1(d). We therefore expect it to be comparable to the cross section for $\eta_c+\eta_{c2}(1D)$.

III. PREDICTIONS FOR B FACTORIES

In this section, we calculate the cross sections for exclusive double-charmonium production in e^+e^- annihilation at the B factories. We also analyze the errors in the prediction for the $J/\psi+J/\psi$ production cross section.

A. Cross sections

The results in Section II were expressed in terms of the ratio R, which is defined in Eq. (1). The corresponding cross sections are

$$\sigma[H_1+H_2]=\frac{4\pi\alpha^2}{3s}R[H_1+H_2]. \qquad (32)$$

The ratios R depend on the coupling constant α, the charm-quark mass m_c, and the NRQCD matrix elements $\langle O_1\rangle_H$.

For the charm-quark mass m_c, we use the next-to-leading-order pole mass, which can be expressed in terms of the running mass $\bar{m}_c(\bar{m}_c)$ as

$$m_c=\bar{m}_c(\bar{m}_c)\left(1+\frac{4}{3}\frac{\alpha_s}{\pi}\right). \qquad (33)$$

If we take the running mass of the charm quark to be $\bar{m}_c(\bar{m}_c)=1.2\pm0.2$ GeV, then the pole mass is $m_c=1.4\pm0.2$ GeV.

TABLE I: The NRQCD matrix elements $\langle O_1 \rangle_H$. H is a charmonium state. These matrix elements are computed in Ref. [4] from electromagnetic annihilation decays, using $m_c = 1.4$ GeV. The errors are the statistical errors associated with the experimental inputs only.

H	η_c, J/ψ	$\eta_c(2S)$, $\psi(2S)$	$h_c(1\mathrm{P})$, $\chi_{cJ}(1P)$	$\eta_{c2}(1D)$, $\psi_1(1D)$
$\langle O_1 \rangle_H$	0.335 ± 0.024 GeV^3	0.139 ± 0.010 GeV^3	0.053 ± 0.009 GeV^5	0.095 ± 0.015 GeV^7

TABLE II: Cross sections in fb for e^+e^- annihilation at $E_{\mathrm{beam}} = 5.3$ GeV into double-charmonium states $H_1 + H_2$ with $C = -1$. The errors are only those from variations in the pole mass $m_c = 1.4 \pm 0.2$ GeV. There are additional large errors associated with perturbative and relativistic corrections, as discussed in the text.

$H_2 \setminus H_1$	J/ψ	$\psi(2S)$	$h_c(1P)$	$\psi_1(1D)$
J/ψ	8.70 ± 2.94	7.22 ± 2.44	$(6.1 \pm 0.9) \times 10^{-3}$	0.79 ± 0.30
$\psi(2S)$		1.50 ± 0.51	$(2.5 \pm 0.4) \times 10^{-3}$	0.33 ± 0.13
$h_c(1P)$			$(0.19 \pm 0.02) \times 10^{-3}$	

The NRQCD matrix element $\langle O_1 \rangle_H$ can be determined phenomenologically from the electromagnetic annihilation decay rate of either H or of a state that is related to H by the heavy-quark spin symmetry. We make use of the values of the matrix elements that were obtained from such an analysis in Ref. [4]. That analysis takes into account the next-to-leading-order QCD corrections to the annihilation rate in the cases of the S- and P-wave states. It obtains the NRQCD matrix elements for the $2S$ and $1D$ states from the electronic decay rates of the $\psi(2S)$ and $\psi_1(1D)$, under the assumption that the mixing between the $2S$ and $1D$ states is negligible. The values of the matrix elements from that analysis are summarized in Table I for the case $m_c = 1.4$ GeV. For different values of m_c, the values in Table I should be multiplied by $(m_c/1.4\,\mathrm{GeV})^{2+2L}$, where $L = 0$, 1, and 2 for S-waves, P-waves, and D-waves, respectively.

Our predictions for double-charmonium cross sections are given in Table II for $C = -1$ states and in Table III for $C = +1$ states. The error bars are those associated with the uncertainty in the pole mass m_c only. The small error bars for the $\eta_c + \eta_c$ cross section in Table III are a consequence of the value of m_c being fortuitously close to a zero in the derivative of the cross section with respect to m_c. Note that the cross sections in Table II are in fb, while those in Table III are in units of 10^{-3} fb. All of the cross sections, except those for which both of the charmonia are in 1^{--} states, are at least 3 orders of magnitude smaller than the $J/\psi + J/\psi$ cross section. The cross sections for the 1^{--} states are dominated by the photon-fragmentation diagrams in Figs. 1(a) and 1(b). For $m_c = 1.4$ GeV, they contribute 87.5% of the $J/\psi + J/\psi$ cross section. The nonfragmentation diagrams in Figs. 1(c) and 1(d) contribute 0.7%, while the interference term contributes 11.8%.

The cross sections for production of double-charmonium states with opposite C-parity were calculated in Refs. [4, 5]. The cross sections at the B-factory energy in Table II of Ref. [4] were calculated using the same NRQCD matrix elements as the cross section in Table I. In spite of the suppression factor of α^2/α_s^2, the predicted cross section for $J/\psi + J/\psi$ is larger than that for $J/\psi + \eta_c$ by about a factor of 3.7. The kinematic enhancement factor that scales as r^{-6} more than compensates for the suppression factor of α^2/α_s^2. Four of the

TABLE III: Cross sections in units of 10^{-3} fb for e^+e^- annihilation at $E_{\rm beam} = 5.3$ GeV into double-charmonium states $H_1 + H_2$ with $C = +1$. The errors are only those from variations in the pole mass $m_c = 1.4 \pm 0.2$ GeV. There are additional large errors associated with perturbative and relativistic corrections, as discussed in the text.

$H_2 \setminus H_1$	η_c	$\eta_c(2S)$	$\chi_{c0}(1P)$	$\chi_{c1}(1P)$	$\chi_{c2}(1P)$	$\eta_{c2}(1D)$
η_c	1.83 ± 0.10	1.52 ± 0.08	0.34 ± 0.04	1.31 ± 0.29	0.48 ± 0.10	0.18 ± 0.02
$\eta_c(2S)$		0.31 ± 0.02	0.14 ± 0.02	0.54 ± 0.12	0.20 ± 0.04	0.07 ± 0.01

powers of r^{-1} come from the enhancement associated with fragmentation processes. The other two powers of r^{-1} come from the fact that the final state $J/\psi(\pm 1) + \eta_c$ violates hadron helicity conservation by one unit. The angular distributions $d\sigma/d|x|$ for $m_c = 1.4$ GeV are shown in Fig. 2. The normalizations are such that the areas under the curves are equal to the integrated cross sections 8.70 fb and 2.31 fb. At $x = 0$, the differential cross section for $J/\psi + J/\psi$ is larger than that for $J/\psi + \eta_c$ by about a factor 2. However the differential cross section for $J/\psi + J/\psi$ is strongly peaked near the beam direction at $x = \pm 0.994$, where it is larger than that for $J/\psi + \eta_c$ by about a factor 16. The reason for the sharp peak is evident from the expression (12) for the limiting behavior as $r \to 0$ with x fixed. As we have already mentioned, this peak in the angular distribution leads to an enhancement factor $\ln(8/r^4)$ in the integrated cross section.

B. Perturbative corrections

The perturbative corrections to the cross section for $J/\psi + J/\psi$ have not yet been calculated. However the perturbative corrections to the dominant photon-fragmentation diagrams in Figs. 1(a) and 1(b) are closely related to the perturbative correction to the electromagnetic annihilation decay rate for $J/\psi \to e^+e^-$, which gives a multiplicative factor

$$\left(1 - \frac{8}{3}\frac{\alpha_s}{\pi}\right)^2 . \tag{34}$$

The perturbative correction to the photon-fragmentation terms in the cross section for $J/\psi + J/\psi$ is just the square of the expression (34). If we choose the QCD coupling constant to be $\alpha_s = 0.25$, which corresponds to a renormalization scale $2m_c$, then the perturbative correction yields a multiplicative factor $(0.79)^4 = 0.39$. The same perturbative correction factor applies to the cross sections for $J/\psi + \psi(2S)$ and $\psi(2S) + \psi(2S)$. This perturbative correction factor applies only to the leading contributions to the cross sections in the limit $r \to 0$. However, since these contributions are dominant, we conclude that the perturbative corrections are likely to decrease the cross sections by about a factor of 3.

C. Relativistic corrections

The prescription for calculating the leading relativistic correction for S-wave charmonium production processes was summarized in Ref. [4]. The leading relativistic correction is conveniently expressed in terms of a quantity $\langle v^2 \rangle_H$ that can be defined formally as a ratio

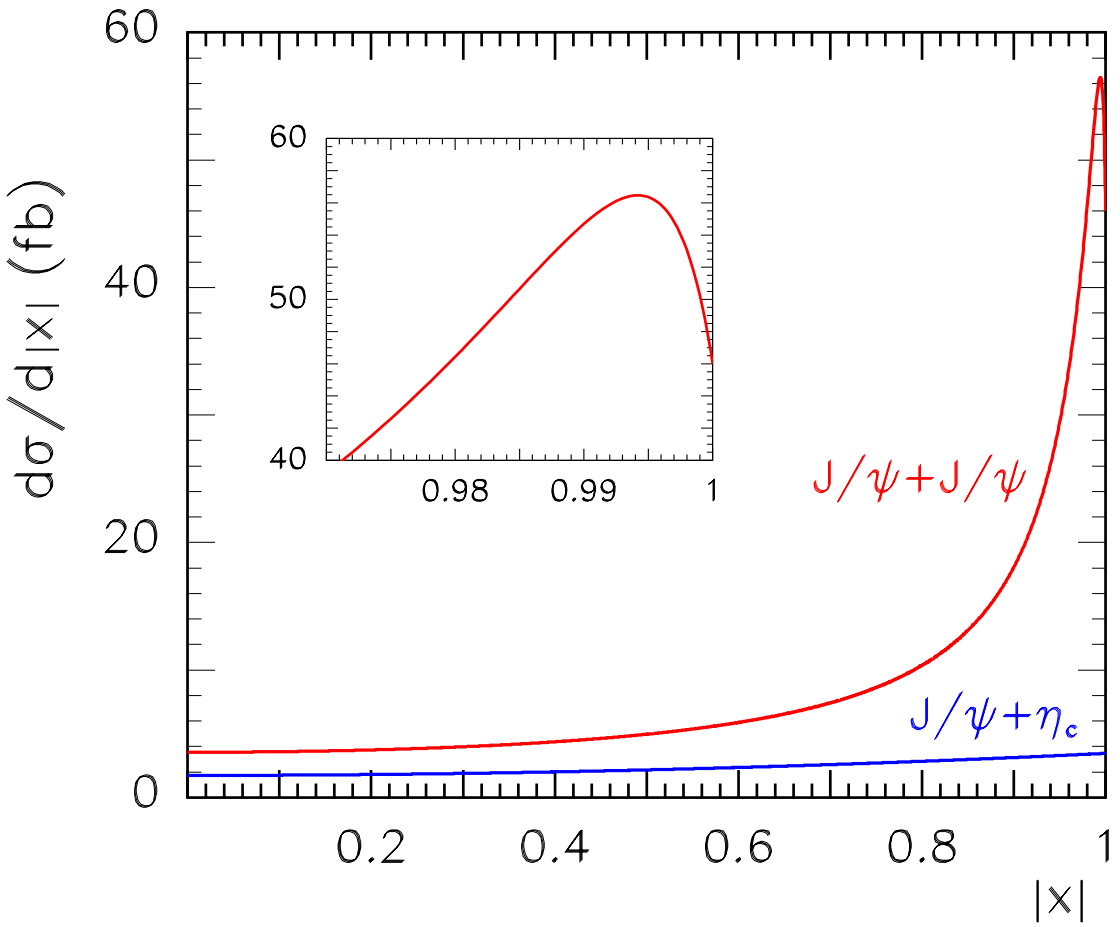

FIG. 2: Differential cross sections $d\sigma/d|x|$ for e^+e^- annihilation at $E_{\rm beam} = 5.3$ GeV into $J/\psi+J/\psi$ and $J/\psi+\eta_c$. There are large errors associated with perturbative and relativistic corrections, as discussed in the text.

of matrix elements in NRQCD. It can also be determined phenomenologically, using the mass M_H of the charmonium state as input [11].

If we keep only the dominant photon-fragmentation contribution to the cross section for $J/\psi + J/\psi$, then the relativistic correction to the cross section is closely related to the relativistic correction to the electromagnetic annihilation decay rate for $J/\psi \to e^+e^-$. The relativistic correction to the photon-fragmentation probability $P_{\gamma\to J/\psi}$ in Eq. (13) is a multiplicative factor

$$\left(1 - \frac{1}{6}\langle v^2\rangle_H\right)^2 \times \left(\frac{2m_c}{M_{J/\psi}}\right)^3. \tag{35}$$

The first factor in the expression (35) arises from the expansion of the electromagnetic current in powers of v [12], while the second factor arises from the dependence of the rate on the charmonium mass, which can be determined from dimensional analysis. The decay rate for $J/\psi \to e^+e^-$ is multiplied by the same factor, except that $2m_c/M_{J/\psi}$ is raised to the power 2 instead of 3. The relativistic correction associated with the phase space for $J/\psi + J/\psi$ can be taken into account by replacing the factor $(1-r^2)^{1/2}$ in Eq. (9) by the expression for $P_{\rm CM}/E_{\rm beam}$ given by Eq. (8). If all of these correction factors are taken into

account, both in the decay rate for $J/\psi \to e^+e^-$ and in $P_{\gamma\to J/\psi}$, then the net effect on the prediction for the production cross section for $J/\psi + J/\psi$ is simply to multiply it by

$$\left(\frac{2m_c}{M_{J/\psi}}\right)^2 \times \frac{P_{\rm CM}/E_{\rm beam}}{(1-r^2)^{1/2}}. \tag{36}$$

For $m_c = 1.4$ GeV, the relativistic corrections decrease the cross sections for $J/\psi + J/\psi$, $J/\psi + \psi(2S)$, and $\psi(2S) + \psi(2S)$ by multiplicative factors of about 0.78, 0.62, and 0.49, respectively. The relativistic corrections also decrease the sensitivity to the value of m_c. The error associated with variations of m_c in the cross section for $J/\psi + J/\psi$ in Table II is about 34% for $m_c = 1.4$ GeV. After we take into account the relativistic correction in (36), this error decreases to about 2%.

The relativistic corrections to the $J/\psi + J/\psi$ cross section are significantly smaller than and have the opposite sign from the relativistic corrections to the $J/\psi + \eta_c$ cross section, which are given in Ref. [4]. For $m_c = 1.4$ GeV, the relativistic corrections to the $J/\psi+\eta_c$ cross section are estimated to increase the cross section by about a factor 5.5. The large difference in the relativistic corrections suggests that there may be large relativistic corrections not only to the absolute cross sections for double-charmonium production, but also to the ratios of those cross sections.

D. Phenomenology

Recently, the Belle Collaboration has measured the cross section for the production of $J/\psi + \eta_c$ by observing a peak in the momentum spectrum of the J/ψ that corresponds to the 2-body final state $J/\psi + \eta_c$ [1]. The measured cross section is

$$\sigma[J/\psi + \eta_c] \times B[\geq 4] = \left(33^{+7}_{-6} \pm 9\right) \text{ fb}, \tag{37}$$

where $B[\geq 4]$ is the branching fraction for the η_c to decay into at least 4 charged particles. Since $B[\geq 4] < 1$, the right side of Eq. (37) is a lower bound on the production cross section for $J/\psi + \eta_c$. This lower bound is about an order of magnitude larger than the predictions of NRQCD in the nonrelativistic limit [4, 5]. The relativistic corrections are large, and they may account for part of the discrepancy [4]. There may also be large nonperturbative corrections to double-charmonium production at the B-factory energy [5]. However the large discrepancy between the predictions and the measurement is still disturbing. In the Belle fit to the J/ψ momentum distribution, the full width at half maximum of the η_c peak is about 0.11 GeV. Since the mass difference between the J/ψ and η_c is about 0.12 GeV, there are probably $J/\psi + J/\psi$ events that contribute to the $J/\psi + \eta_c$ signal that is observed by Belle. If these were taken into account, they would increase the compatibility between the NRQCD prediction of the cross section and the Belle measurement.

The signal for the production of $J/\psi+X$, with m_X near the mass of the η_c, can be resolved into the contributions from $J/\psi+\eta_c$ and from $J/\psi+J/\psi$. One way to do this is to measure the angular distribution of the production products and fit to a linear combination of the angular distributions in Fig. 2. This method tests not only the predicted production rates, but also the dominance of the photon-fragmentation production mechanism. Alternatively, one can measure directly the rate for the production of $J/\psi + J/\psi$ with subsequent decay of both J/ψ's into lepton pairs. In the analysis of Ref. [1], the data set for $J/\psi + X$, with m_X near the mass of the η_c, contains only 67 ± 13 events. Since the branching fraction

for J/ψ into e^+e^- or $\mu^+\mu^-$ is only about 0.12, that data sample may not be large enough to allow one to employ this method. However, as the integrated luminosity increases, the double-dilepton signal should become observable.

The Belle Collaboration also saw evidence for $J/\psi + \chi_{c0}(1P)$ and $J/\psi + \eta_c(2S)$ events. The $\eta_c(2S)$ was recently discovered by the Belle Collaboration at a mass of $M_{\eta_c(2S)} = 3654 \pm 6 \pm 8$ MeV [13]. Since the mass difference between the $\psi(2S)$ and the $\eta_c(2S)$ is only about 0.03 GeV, any signal for $J/\psi + \eta_c(2S)$ in the J/ψ momentum spectrum is probably also contaminated by $J/\psi + \psi(2S)$ events. A 3-peak fit to the momentum spectrum of the J/ψ by the Belle Collaboration gives approximately 67, 39, and 42 events with an accompanying η_c, $\chi_{c0}(1P)$, or $\eta_c(2S)$, with an uncertainty of 12-15 events. The predictions in Ref. [4] for the relative cross sections for the production of a J/ψ with an accompanying η_c, $\chi_{c0}(1P)$, or $\eta_c(2S)$ are 1.00, 0.99, and 0.42, respectively. The observed proportion of events is only marginally compatible with the NRQCD predictions. If significant fractions of the $J/\psi + \eta_c$ and $J/\psi + \eta_c(2S)$ signals are actually $J/\psi + J/\psi$ and $J/\psi + \psi(2S)$ events, then the data would be more compatible with the NRQCD predictions.

In summary, we have calculated the cross sections for e^+e^- annihilation through two virtual photons into exclusive double-charmonium states. The cross sections are particularly large if the two charmonia are both 1^{--} states. In the absence of radiative and relativistic corrections, the predicted cross section for the production of $J/\psi + J/\psi$ at the B factories is larger than that for $J/\psi + \eta_c$ by a factor of about 3.7. The perturbative and relativistic corrections for these two processes may be rather different and could significantly change the prediction for the ratio of the cross sections. Nevertheless, the inclusion of contributions from processes involving two virtual photons in the theoretical prediction for the cross section for $J/\psi + \eta_c$ production is likely to decrease the large discrepancy between that prediction and the Belle measurement.

Acknowledgments

One of us (E.B.) would like to thank B. Yabsley for valuable discussions. The research of G.T.B. and J.L. in the High Energy Physics Division at Argonne National Laboratory is supported by the U. S. Department of Energy, Division of High Energy Physics, under Contract W-31-109-ENG-38. The research of E.B. is supported in part by the U. S. Department of Energy, Division of High Energy Physics, under grant DE-FG02-91-ER4069 and by Fermilab, which is operated by Universities Research Association Inc. under Contract DE-AC02-76CH03000 with the U. S. Department of Energy.

---

[1] K. Abe *et al.* [Belle Collaboration], Phys. Rev. Lett. **89**, 142001 (2002) [arXiv:hep-ex/0205104].

[2] G. T. Bodwin, E. Braaten, and G. P. Lepage, Phys. Rev. D **51**, 1125 (1995); **55**, 5853(E) (1997) [arXiv:hep-ph/9407339].

[3] M. B. Einhorn and S. D. Ellis, Phys. Rev. D **12**, 2007 (1975); S. D. Ellis, M. B. Einhorn, and C. Quigg, Phys. Rev. Lett. **36**, 1263 (1976); C. E. Carlson and R. Suaya, Phys. Rev. D **14**, 3115 (1976); J. H. Kühn, Phys. Lett. B **89**, 385 (1980); T. A. DeGrand and D. Toussaint, Phys. Lett. B **89**, 256 (1980); J. H. Kühn, S. Nussinov, and R. Rückl, Z. Phys. C **5**, 117 (1980); M. B. Wise, Phys. Lett. B **89**, 229 (1980); C.-H. Chang, Nucl. Phys. B **172**, 425

(1980); R. Baier and R. Rückl, Phys. Lett. B **102**, 364 (1981); E. L. Berger and D. Jones, Phys. Rev. D **23**, 1521 (1981); W. Y. Keung, in *The Cornell Z^0 Theory Workshop*, edited by M. E. Peskin and S.-H. Tye (Cornell University, Ithaca, 1981).

[4] E. Braaten and J. Lee, Phys. Rev. D (to be published), arXiv:hep-ph/0211085.

[5] K.-Y. Liu, Z.-G. He, and K.-T. Chao, arXiv:hep-ph/0211181.

[6] G. T. Bodwin, J. Lee, and E. Braaten, Phys. Rev. Lett. (to be published), arXiv:hep-ph/0212181.

[7] V. L. Chernyak and A. R. Zhitnitsky, Sov. J. Nucl. Phys. **31**, 544 (1980) [Yad. Fiz. **31** (1980) 1053].

[8] S. J. Brodsky and G. P. Lepage, Phys. Rev. D **24**, 2848 (1981).

[9] S. Fleming, Phys. Rev. D **50**, 5808 (1994) [arXiv:hep-ph/9403396].

[10] C.-H. Chang, C.-F. Qiao, and J.-X. Wang, Phys. Rev. D **56**, 1363 (1997) [arXiv:hep-ph/9704364]; Phys. Rev. D **57**, 4035 (1998).

[11] M. Gremm and A. Kapustin, Phys. Lett. B **407**, 323 (1997) [arXiv:hep-ph/9701353].

[12] E. Braaten and Y.-Q. Chen, Phys. Rev. D **57**, 4236 (1998); **59**, 079901(E) (1999) [arXiv:hep-ph/9710357].

[13] S.-K. Choi *et al.* [Belle Collaboration], Phys. Rev. Lett. **89**, 102001 (2002); **89**, 129901(E) (2002) [arXiv:hep-ex/0206002].